Materials Sciences and Applications, 2015, 6, 228-233
Published Online March 2015 in SciRes. http://www.scirp.org/journal/msa
http://dx.doi.org/10.4236/msa.2015.63027

Scientific Research Publishing

The Role of Silver Additions in Formation of Sn-Bi-Ag Semiconductor Alloys by Rapid Solidification

Tarek El Ashram[1,2]

[1]Physics Department, Faculty of Science, Port Said University, Port Said, Egypt
[2]Physics Department, Preparatory Year Deanship, Jazan University, Jazan, Kingdom of Saudi Arabia
Email: tnelashram@gmail.com

Received 13 February 2015; accepted 4 March 2015; published 10 March 2015

Copyright © 2015 by author and Scientific Research Publishing Inc.
This work is licensed under the Creative Commons Attribution International License (CC BY).
http://creativecommons.org/licenses/by/4.0/

Open Access

Abstract

Five alloys Sn-5Bi-xAg (x = 0, 1, 2, 3, and 4 in at %) are produced by rapid solidification using melt-spinning technique. From temperature dependence of electrical resistivity (TDR), it is found that the Sn-5Bi-xAg (x = 1, 2, 3, 4 in at %) rapidly solidified by melt spinning technique are narrow band semiconductor alloys. The energy gap E_g decreases by increasing Ag concentration from 203 meV for Sn-5Bi-1Ag to 97.5 meV for Sn-5Bi-4Ag alloy. From x-ray diffraction analysis (XRD), it is found that the Hume-Rothery condition for phase stability is not satisfied for this alloy.

Keywords

Rapid Solidification, Semiconductor, Energy gap, Resistivity, Sn-Bi-Ag Alloys

1. Introduction

The production of semiconductor alloys by rapid solidification is simple, uncomplicated and economic. By this method, we can directly obtain thin semiconductor wafers available for manufacturing semiconductor devices. Also, the semiconductors prepared by rapid solidification exhibit considerable improvements over alloys made from conventional materials. The thermoelectric materials fabricated by rapid solidification displayed a high figure of merit [1]. Rapid solidification prevents rejection of extra solute atoms and thus prevents precipitation from a solid solution, which in turn increases the solid solubility. The production of semiconductor alloys by rapid solidification depends mainly on the type of alloy system used. Most of these alloys are based on group V, such as Bi. The solute atoms play an important role in formation of semiconductors by rapid solidification. In

How to cite this paper: El Ashram, T. (2015) The Role of Silver Additions in Formation of Sn-Bi-Ag Semiconductor Alloys by Rapid Solidification. *Materials Sciences and Applications*, **6**, 228-233. http://dx.doi.org/10.4236/msa.2015.63027

this respect, a series of rapidly solidified Bi based semiconductor alloys were produced using melt spinning technique [2]-[4]. They found that the semiconducting behavior depended on the type of the solute atoms added to Bi. The alloys contain solute atoms with odd valencies such as Ag (+1), Al (+3) and Sb (+5) have semiconducting behavior by contrast all alloys contain solute atoms with even valencies such as Zn (+2) and Sn (+4) have metallic behavior. The produced semiconductor alloys are narrow band semiconductors. The band gap was decreased by increasing valency from 225.1 meV for Bi-Ag system to 12.7 meV for Bi-Sb system. Also some alloys based on Bi, such as Bi-Sb were found to be semiconductors even though they were produced by conventional methods [5]-[7]. It was found by [8] that by alloying Bi with Sn, a large increase in resistivity was obtained and the temperature coefficient of resistivity was found to be zero. The present work is an attempt to study the effect of rapid solidification on the electrical properties of alloy system based on an element in group IV such as tin (β-Sn). Group IV contains the elemental semiconductors Si, Ge, and α-Sn, (the allotrope of Sn stable below 13.2˚C). The three previous semiconductor elements Si, Ge and α-Sn have the same crystal structure which is diamond cubic. β-Sn (the stable allotrope of Sn above 13.2˚C) is metallic and its crystal structure is body centered tetragonal. Pure tin (β-Sn) was rapidly solidified using melt spinning technique and no amorphous or non-equilibrium crystalline phases was formed [9]. Also it was found that its resistivity at room temperature was increased and its temperature coefficient of resistivity (TCR) was decreased in comparison with conventional pure β-Sn. Therefore, the aim of the present work is to study the effect of rapid solidification using melt spinning technique on the structure and electrical properties of Sn-Bi. Also the effect of silver (Ag) additions on the structure and electrical properties of Sn-Bi alloy will be studied.

2. Experimental Procedures

The materials used in the present work were Sn, Bi, fragments and Ag wires, the starting purity were better than 99.99%. Five alloys Sn-5Bi-xAg (x = 0, 1, 2, 3, and 4 in at %) were produced by a single copper roller (200 mm in diameter) melt spinning technique. The process parameters such as the ejection temperature, and the linear speed of the wheel were fixed at 873 K and 30.4 ms^{-1} respectively. X-ray diffraction analysis (XRD) was carried out with a XPERT-PRO X-ray diffractometer, using Cu-K_α radiation (λ = 1.5406 Å). Differential Scanning Calorimetry (DSC) was carried out in a Shimadzu (DSC-60) with heating rate 10 K·min^{-1}. The temperature dependence of resistivity (TDR) was measured by four probe method using microhmmeter of type BS407. The BS407 uses a four terminal measurement system via high quality Kelvin Clip leads with sensitivity is 1 μΩ. The heating range starts from room temperature up to 530 K with heating rate about 5 K·min^{-1}.

3. Results and Discussion

3.1. Structure

Figure 1 shows the x-ray diffraction XRD patterns for as-quenched melt-spun Sn-5Bi-xAg, (x = 0, 1, 2, 3, and 4 in at %) alloys. The XRD for Sn-5Bi alloy is shown in **Figure 1(a)**, Bi is precipitated as indicated by (012) peak and all the other peaks are for Sn. The matrix is β-Sn solid solution, the unit cell of β-Sn is body centered tetragonal ($I4_1$/amd).The crystal structure of Bi is rhombohedral-hexagonal (S.G.: R3m) with $\boldsymbol{a}$ = 4.5491, $\boldsymbol{c}$ = 11.9485 Å.

Figure 1(b) shows for Sn-5Bi-1Ag alloy the same structure, *i.e.* precipitation of Bi in the Sn matrix as indicated by (012) peak. For Sn-5Bi-2Ag alloy (**Figure 1(c)**) the peak due to Bi is disappeared and instead a peak due to Ag_3Sn (211) is appeared. As the Ag concentration increases the intensity of the peak due to Ag_3Sn increases (**Figure 1(d)** and **Figure 1(e)**). The crystal structure of Ag_3Sn is orthorhombic (S.G.: Pmmn) with lattice parameters $\boldsymbol{a}$ = 5.9680, $\boldsymbol{b}$ =4.7802, and $\boldsymbol{c}$ =5.1843. The detail of XRD analysis is shown in **Table 1**.

The axial ratio $\boldsymbol{c/a}$ is very important parameter in determination the properties of Sn-based alloys since the work of [10]. **Figure 2(a)** shows the variation of the axial ratio $\boldsymbol{c/a}$ with Ag concentration. The lattice parameters $\boldsymbol{a}$, $\boldsymbol{c}$, and the axial ratio $\boldsymbol{c/a}$ for pure Sn rapidly solidified were found by [9] to be 5.809 Å, 3.169 Å, and 0.5455 respectively.

The addition of Bi to Sn expands the β-Sn tetragonal unit cell, both $\boldsymbol{a}$ and $\boldsymbol{c}$ are increased (see **Table 1**) and the $\boldsymbol{c/a}$ ratio is decreased in agreement with [10]. It is evident that the addition of Ag increases the axial ratio from 0.5436 to 0.5464 in agreement with [10]. Since low valency atom like Ag increases the axial ratio of β-Sn tetragonal unit cell and high valency atom decreases it. **Figure 2(b)** shows the variation of the volume of the

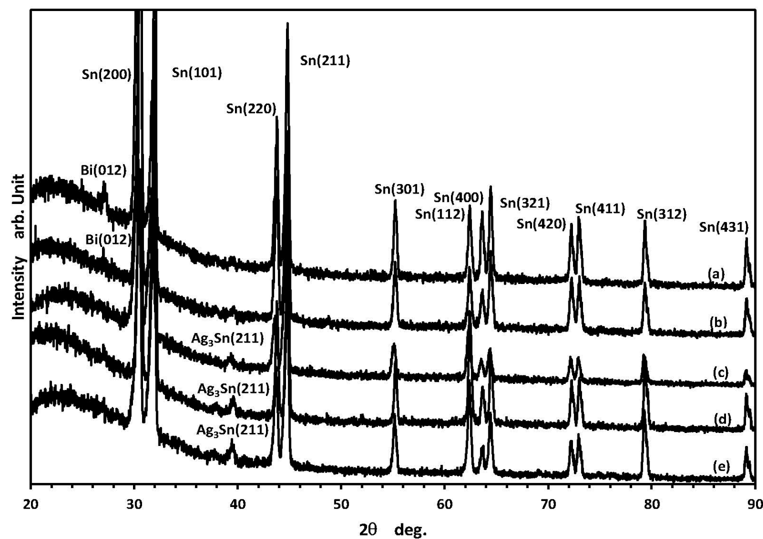

Figure 1. The XRD patterns for as-quenched melt-spun alloys. (a) Sn-5Bi; (b) Sn-5Bi-1Ag; (c) Sn-5Bi-2Ag; (d) Sn-5Bi-3Ag; and (e) Sn-5Bi-4Ag in at %.

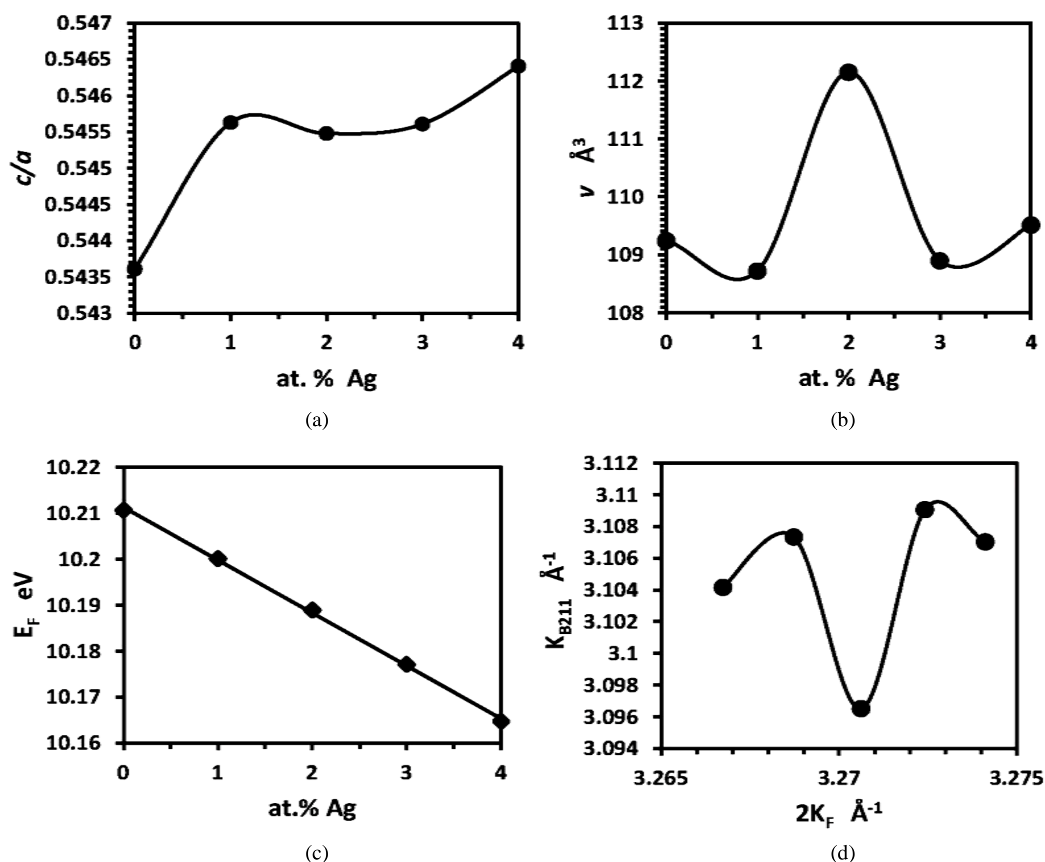

Figure 2. (a) The variation of ***c/a*** with Ag concentration; (b) The variation of ***v*** with Ag concentration; (c) The variation of E_F with Ag concentration; and (d) The variation of K_{B211} with k_F.

unit cell ***v*** of the β-Sn matrix with Ag concentration. The volume of unit cell has a maximum value 112.15 $Å^3$ at 2 at % Ag. **Figure 2(c)** shows the variation of Fermi energy E_F with Ag concentration. It is evident that Fermi-energy decreases by increasing Ag concentration from 10.21 eV to 10.16 eV. This decrease is due to that Ag

Table 1. The x-ray diffraction details for as-quenched melt spun Sn-5Bi-xAg (x = 0, 1, 2, 3, and 4 in at %) alloys.

Alloy	Phases present in Sn	hkl	The lattice parameters of the β-Sn matrix				Crystal structure
			a **Å**	***c*** **Å**	***c/a***	***v*** **Å^3**	
Sn-5Bi	Bi	(012)	5.8573	3.1841	0.5436	109.24	Rho.-hex. (S.G.: $R\bar{3}m$)
Sn-5Bi-1Ag	Bi	(012)	5.8407	3.1868	0.5456	108.71	Rho.-hex. (S.G.: $R\bar{3}m$)
Sn-5Bi-2Ag	Ag_3Sn	(211)	5.9021	3.2194	0.5454	112.15	Ortho. (S.G.: Pmmn)
Sn-5Bi-3Ag	Ag_3Sn	(211)	5.8440	3.1885	0.5456	108.89	Ortho. (S.G.: Pmmn)
Sn-5Bi-4Ag	Ag_3Sn	(211)	5.8522	3.1976	0.5464	109.51	Ortho. (S.G.: Pmmn)

atom with valency +1 replaces Sn atom with valency +4. **Figure 2(d)** shows the variation of the diameter of Brillouin zone K_{B211} in the (211) direction with the diameter of Fermi sphere $2k_F$. It is evident that the Hume-Rothery condition for phase stability is not satisfied for this alloy.

3.2. Thermal Analysis

Figure 3 shows the DSC curves for as-quenched melt-spun pure Sn-5Bi-x Ag (x = 0, 1, 2, 3, and 4 in at %) alloys. A transition occurs at about 413 K for all alloys; however the endothermic peak for this transition decreases by increasing Ag concentration. This transition may be due to the eutectic reaction which starts at 413 K. Finally, the endothermic peak due to melting was obtained, from which the melting temperature T_m and the enthalpy of fusion ΔH_m have been determined. ΔH_m was obtained from the integral under the DSC peak of melting as given by Equation (1);

$$\Delta H_m = \int_{T_0}^{T_f} C_p \mathrm{d}T \tag{1}$$

where; C_p is the heat capacity at constant pressure, T_0 and T_f are known as onset melting temperature and final melting temperature of the specimen, respectively. **Table 2** shows the detail of the DSC results. It is evident that the melting temperature decreases by increasing Ag concentration from 492.29 K for Sn-5Bi to 483.58 K for Sn-5Bi-4Ag. The enthalpy of fusion ΔH_m decreases by increasing Ag concentration from 57.27 $kJ \cdot kg^{-1}$ for Sn-5Bi to 47.5 $kJkg^{-1}$ for Sn-5Bi-3Ag.

3.3. Electrical Properties

Figure 4(a) shows the temperature dependence of resistivity obtained for as-quenched melt-spun Sn-5Bi alloy in the temperature range from 300 to 500 K. The behavior is metallic *i.e.* the resistivity increases by increasing temperature. The resistivity at room temperature ρ is found to be 4.56×10^{-6} Ωm.

The resistivity at room temperature for pure Sn rapidly solidified was found to be 0.166×10^{-6} Ωm [5]. This means that the addition of Bi causes large increase in the resistivity. This increase in the resistivity is attributed to two reasons; the first is the presence of Bi atoms in Sn lattice which acts as a scattering center for the conduction electrons. The second is due to the precipitation of Bi as a distinct phase which has high resistance (2.09 x 10^{-6} Ωm) according to [3]. The temperature coefficient of resistivity TCR was calculated to be 9.15×10^{-3} K^{-1} (see **Table 3**). The TCR is increased due to the addition of Bi since TCR for pure Sn rapidly solidified was found to be 3.23×10^{-3} K^{-1} [9].

Figure 4(b) shows the temperature dependence of resistivity (TDR) obtained for as-quenched melt-spun Sn-5Bi-xAg (x = 1, 2, 3, and 4 in at %) alloys. It is evident that the behavior is semiconducting for all alloys containing Ag *i.e.* the resistivity decreases by increasing temperature. The variation of resistivity at room temperature ρ with Ag concentration is shown in **Figure 4(c)**. The resistivity at room temperature ρ decreases by increasing Ag concentration. This decrease in resistivity can be attributed to the increase in the axial ratio ***c/a*** due the addition of Ag as shown in **Figure 2(a)**. The energy gap E_g was calculated for the semiconducting alloys and the result is shown in **Figure 4(d)**. The energy gap E_g decreases by increasing Ag concentration from 203 meV for Sn-5Bi-1Ag to 97.5 meV for Sn-5Bi-4Ag (see **Table 3**). The semiconducting behavior may be explained as the following; both Bi and Ag atoms are dissolved in Sn lattice, the Ag atoms provide a donor level near the conduction band. Electrons from this level are raised to the conduction band by thermal agitation. Therefore the total number of carriers increases with temperature which in turn decreases the resistivity.

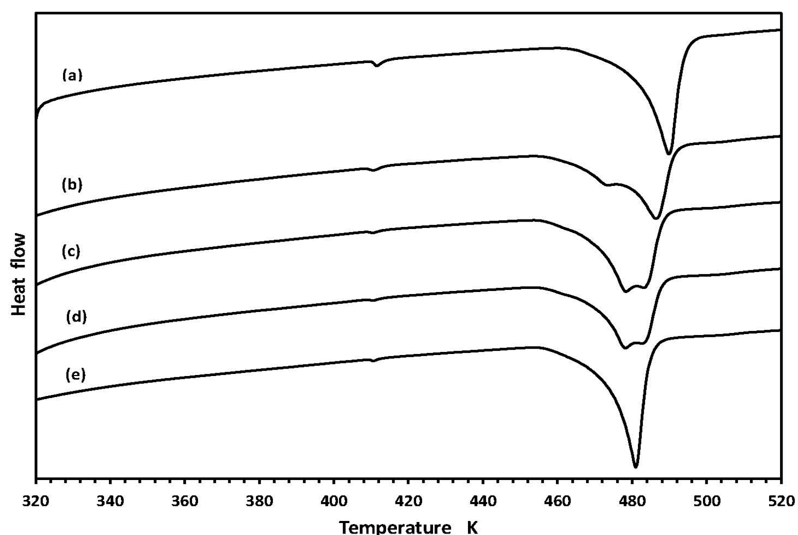

Figure 3. The DSC curves for as-quenched melt-spun alloys. (a) Sn-5Bi; (b) Sn-5Bi-1Ag; (c) Sn-5Bi-2Ag; (d) Sn-5Bi-3Ag, and (e) Sn-5Bi-4Ag in at %.

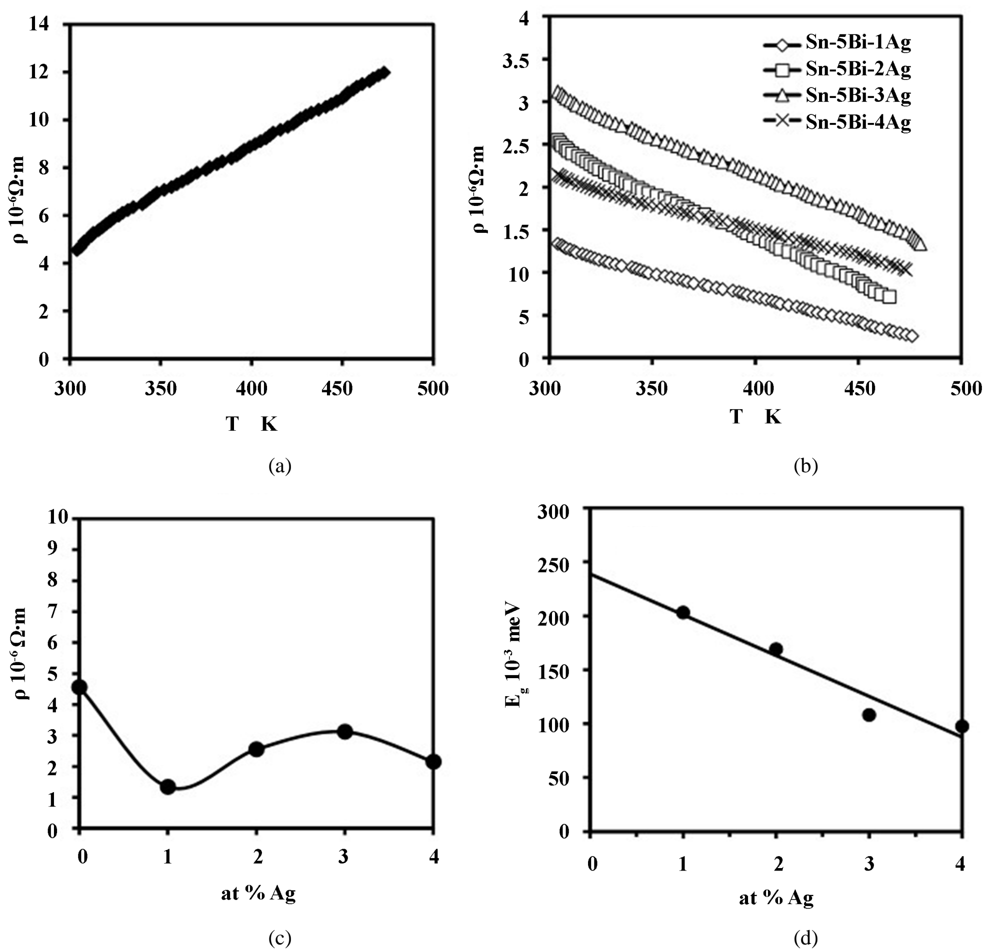

Figure 4. (a) The TDR for Sn-5Bi alloy; (b) The TDR for as-quenched melt-spun Sn-5Bi-xAg (x = 1, 2, 3, and 4 in at %) alloys; (c) The variation of ρ at room temperature with Ag concentration; (d) The variation of E_g with Ag concentration.

Table 2. The DSC details for as-quenched melt spun pure Sn-5Bi-xAg (x = 0, 1, 2, 3, and 4 in at %) alloys.

Alloy	T_m K	ΔH_m $kJ \cdot kg^{-1}$
Sn-5Bi	492.29	57.27
Sn-5Bi-1Ag	488.88	48.58
Sn-5Bi-2Ag	485.64	52.92
Sn-5Bi-3Ag	485.70	47.50
Sn-5Bi-4Ag	483.58	61.09

Table 3. The results of electrical measurements for as-quenched melt-spun Sn-5Bi-x Ag (x = 0, 1, 2, 3, and 4 in at %) alloys.

Alloy	$\rho \times 10^{-6}$ Ωm at room temp.	Behavior	TCR $\times 10^{-3}$ (K^{-1})	E_g (meV)
Sn-5Bi	4.56	Metallic	9.15	
Sn-5Bi-1Ag	1.34	Semiconducting		203
Sn-5Bi-2Ag	2.55	Semiconducting		169
Sn-5Bi-3Ag	3.12	Semiconducting		108
Sn-5Bi-4Ag	2.15	Semiconducting		97.5

4. Conclusion

From above, it is clear that rapidly solidified semiconductors based on Sn-Bi can be produced after the ternary addition of Ag. Since from temperature dependence of electrical resistivity (TDR), it is found that the Sn-5Bi-xAg (x = 1, 2, 3, 4 in at %) rapidly solidified by melt spinning technique are narrow band semiconductor alloys. The energy gap E_g decreases by increasing Ag concentration from 203 meV for Sn-5Bi-1Ag to 97.5 meV for Sn-5Bi-4Ag. Also from X-ray diffraction analysis (XRD), it is found that Hume-Rothery condition for phase stability is not satisfied for this alloy.

References

[1] Horio, Y., Yamashita, H. and Hayashi, T. (2004) Microstructure and Thermoelectric Properties of Hot-Pressed p-Type $Bi_{0.5}Sb_{1.5}Te_3$ Alloys Prepared by Rapid Solidification Technique. *Materials Transactions*, **45**, 3309-3313. http://dx.doi.org/10.2320/matertrans.45.3309

[2] Raouf A., Kamal M., El Ashram T. and Mosaad S. (2010) Rapidly Solidified Semiconducting Bi-Ag Alloys Produced Using Melt-Spinning Technique. *Journal of Ovonic Research*, **6**, 297-302.

[3] El-Ashram T., Kamal, M., Raouf, M.A. and Mosaad, S. (2012) Odd Valency Dopants Convert Bismuth into Semiconductor. *Journal of Ovonic Research*, **8**, 97-104.

[4] EL-Ashram T. (2015) Formation of Supersaturated Solid Solutions Bi-Ag and Bi-Zn by Rapid Solidification Using Melt Spinning Technique. *Materials Sciences and Applications*, **6**, 183-188. http://dx.doi.org/10.4236/msa.2015.62021

[5] Dutta, S., Shubha, V., Ramesh, T.G. and D'Sa, F. (2009) Thermal and Electronic Properties of Bi1-xSbx Alloys. *Journal of Alloys and Compounds*, **467**, 305-309. http://dx.doi.org/10.1016/j.jallcom.2007.11.146

[6] Lenoira, B., Dauscher, A., Cassartb, M., Ravichc, Y.I. and Scherrer, H. (1998) Effect of Antimony Content on the Thermoelectric Figure of Merit of Bi1-xSbx Alloys. *Journal of Physics and Chemistry of Solids*, **59**, 129-134. http://dx.doi.org/10.1016/S0022-3697(97)00187-X

[7] Lenoira, B., Cassartb, M., Michenaud, J.P., Scherrer, H. and Scherrer, S. (1996) Transport Properties of Bi-rich Bi-Sb Alloys. *Journal of Physics and Chemistry of Solids*, **57**, 89-99. http://dx.doi.org/10.1016/0022-3697(95)00148-4

[8] Kamal, M. and El-Ashram, T. (2008) Zero and Negative Temperature Coefficients of Resistivity of Rapidly Solidified Bi-Sn Alloys Using Melt-Spinning Technique. *Journal of Materials Science*: *Materials in Electronics*, **19**, 91-96. http://dx.doi.org/10.1007/s10854-007-9315-4

[9] El-Ashram T. (2006) The Structure and Properties of Rapidly Solidified Pure Tin. *Radiation Effects and Defects in Solids*, **161**, 193-197.

[10] El-Ashram T. (2005) The Relation between Valency, Axial Ratio, Young's Modulus and Resistivity of Rapidly Solidified Tin-Based Eutectic Alloys. *Journal of Materials Science*: *Materials in Electronics*, **16**, 501-505. http://dx.doi.org/10.1007/s10854-005-2724-3